RSC Advances

ROYAL SOCIETY OF CHEMISTRY

www.rsc.org/advances

Individual Based Modeling of *Pseudomonas aeruginosa* Biofilm with Three Detachment Mechanisms

Cheng Li [a,b], Yilei Zhang [a#], Cohen Yehuda[b]

School of Mechanical & Aerospace Engineering, Nanyang Technological University, Singapore[a]

Singapore Centre on Environmental Life Sciences Engineering, Nanyang Technological University, Singapore[b]

Running Head: Modeling of Biofilms with Detachment

#Correspondence to Yilei Zhang, YLZhang@ntu.edu.sg

Abstract

Individual based simulation approach has attracted more and more interests in biofilm simulation. Different from the conventional biomass based simulation method, detachments are not available in many individual based simulation packages. In this paper, three detachment mechanisms were successfully integrated into an individual-based modeling package (iDynoMiCs). With the new capabilities, the influence of bacterial detachment on *Pseudomonas aeruginosa* biofilm was studied. The simulated results agreed well with previous reports, including the effect of shear detachment on smoothening biofilms, nutrient-limited detachment on hollowing the biofilms, and erosion detachment on isolating bacterial clusters. New findings are also discovered including the effects of different detachment mechanisms on the equilibrium state, time-dependent effects of each detachment mechanism on biofilm structure, sensitivity of the detachment coefficient values, etc.

Keywords

iDynoMiCs, biofilm development, bacterial detachment, *Pseudomonas aeruginosa*

Introduction

Bacterial attachment to surfaces and formation of biofilms are important for processes like wastewater treatment (WWT) (1,2), bacterial infection (3,4), etc. Study of biofilm structure formation could be critical for both constructing robust biofilms and eradicating undesired biofilms depending on applications and requirements. Biofilm structure can influence biofilm growth in various aspects. One important example is that it can change the transportation of nutrient and waste products as well as the mechanical stability of the biofilm (5). With the development of microscopy technology, biofilm structures can nowadays be viewed directly under confocal laser scanning microscope (CLSM). Many studies have been done to investigate the effect of different factors on biofilm structure formation (6–8). However, the mechanisms behind the formation of complex biofilm structures under different conditions are still not very well elaborated and much work still need to be done probably because many factors are involved, such as substrate concentration (9,10), attachment surface, which is the surface for bacterial attachment and biofilm formation, properties (11,12), bacterial detachment and motility (13–15). Among all these factors, bacterial detachment is widely believed to affect biofilm structure significantly. The final steady state of biofilm structure is the result of bacterial growth balanced by detachment events (15–17). Detachment of multiple bacterial cells could reshape the biofilm and change its spatial heterogeneity (15). Reattachment of detached bacteria was suggested as one cause for the formation of higher-level biofilm structures (18).

Bacterial detachment under no human interruption can be divided into two main groups: continuous process and sloughing process (15). Two major methods have been applied to study bacterial continuous detachment process. One is using simplified but classical equations to calculate the detachment rate or probability. Three processes, shear detachment referring to fluid shear effect, nutrient-limited detachment referring to nutrient limitation effect, and erosion detachment indicating surface cell escape from the surface effect, have been proposed to take all detachment causes into consideration (19). The other method is to determine detachment according to the calculated biofilm internal shear stress (20,21), which requires a good knowledge of the biofilm mechanical properties and parameters like Young's modulus and Poisson's ratio. Usually the sloughing detachment process, which could be defined as the large detachment of biomass in a short time period, is treated as a result of other detachment processes rather than an implemented mechanism, thus, not explicitly included in biofilm models.

In the current study, we integrated the previously discussed three detachment mechanisms (19) into an individual-based modeling (IBM) software – individual-based dynamics of microbial communities simulator (iDynoMiCs), which is an open source software governed by CeCILL license under French law and was developed by a group of researchers (22), in order to study the influence of detachment on biofilm structure formation. Codes with ability to extract quantitative parameters, including thickness, roughness, enlargement, and cell number, from simulation results for biofilm establishment characterization were also developed, which are available to public upon request. Replicates were obtained by changing initial conditions (number and locations of bacteria) which made the results more convincing and reliable.

With the added capabilities, we quantified the effects of the three mechanisms on biofilm structures systematically, which is different from the previous work (19) that applied the mechanisms using biomass-based modeling (BBM) method. The IBM method is preferred because of the two important advantages compared with the BBM method. First, different cells could have different growth parameters and detachment can be made based on cells using the IBM method whereas detachment can only be made based on grids for the BBM method. Second, continuous displacement can be achieved in the IBM method while displacement can only be made from grid to grid discretely for the BBM method (6,23,24). As a result, a more systematic and realistic biofilm simulation environment was established, which could enhance fundamental understanding in biofilm development and better guide experimental design and analysis of biofilm studies.

Materials and Methods

Individual-based Dynamics of Microbial Communities Simulator (iDynoMiCs)

In iDynoMiCs, biofilm structures are developed from the growth and movement of single bacterium. Overall biofilm reactor is divided into three subparts in the model, including the bulk fluid, the boundary layer, and the solid biofilm (Figure 1). In the bulk fluid, the medium is considered to be totally mixed and no substrate gradient exists. In the boundary layer, only diffusion exists and substrate gradients start to be generated. While in the biofilm, both diffusion and reaction are considered at the same time and the substrate diffusivity is different from what in the boundary layer. The simulation process contains several stages: bacterial initial attachment, bacterial growth and division, bacterial detachment and dispersal, and bacterial death.

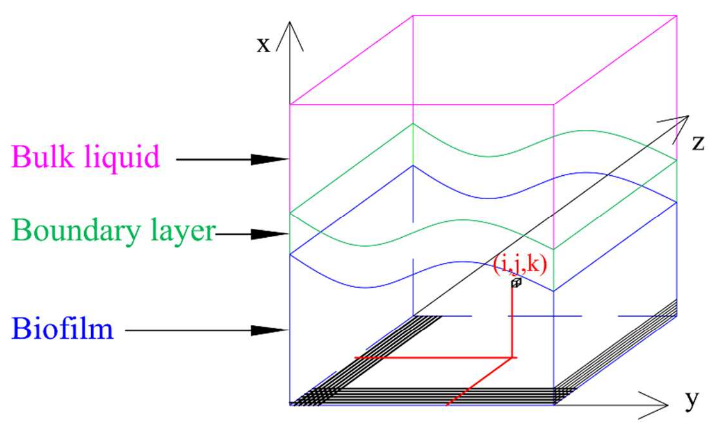

Figure 1. Computational domain illustration ((i,j,k) is the grid reference for the bacterium)

The whole simulation domain is divided into small grids and the simulation cycle could be roughly divided into the following three major steps: first is substrate concentration calculation in each grid based on diffusion reaction processes (Equation 1) from bulk fluid to biofilm; second is bacterial biomass growth (Equation 2) and division when threshold diameter is reached as well as biofilm internal pressure release by moving cells apart according to defined algorithm; last is to process bacterial detachment. Then the cycle is restarted from the first step. Attention should be paid that substrate concentration is considered constant when calculating the biomass growth and biofilm is considered to be static when calculating the substrate concentration due to the different time scales, for example, biomass growth is very slow compared with substrate diffusion. More details regarding the software could be found in literatures (22,25,26).

$$\frac{\partial s}{\partial t} = D\left(\frac{\partial s^2}{\partial^2 x} + \frac{\partial s^2}{\partial^2 y} + \frac{\partial s^2}{\partial^2 z}\right) + r_s \quad (1)$$

$$\mu = \mu_{\max} \frac{s}{K_s + s} \quad (2)$$

where s is the substrate concentration, r_S is the substrate reaction rate, D is the substrate diffusion coefficient, μ is the biomass specific growth rate, $\mu_{\max}$ is the biomass maximum specific growth rate, and K_S is the substrate half-saturation coefficient. Substrate consumption rate can be calculated by $r_S = \mu / Y_S$ where Y_S is the yield coefficient of biomass production on substrate consumption.

Detachment Mechanisms

Previous detachment mechanism used in iDynoMiCs, which was called erosion, was related solely to biofilm thickness or biomass concentration, which was not enough because other factors like nutrient concentration can influence detachment as well. In this study, three different detachment mechanisms adopted from the BBM method (19) was integrated into iDynoMiCs as discussed in the following.

Shear detachment

Shear detachment refers to the detachment caused mainly by fluid shear stress. Previous studies (17,19) have proved that the effect of fluid shear on bacterial detachment could be simplified as a quadratic function of the biofilm local thickness with acceptable accuracy. Therefore, instead of applying the complex fluid dynamics into simulation directly, quadratic function is used as an effective simplification in current model. The detachment probability of bacteria caused by shear (P_{ds}) is modeled as:

$$P_{ds} = K_{ds} \cdot \Delta t \cdot \left(\frac{h_i}{h_{\max}} \right)^2 \tag{3}$$

where K_{ds} is the detachment coefficient, Δt is the simulation time step, i is a reference of the specific cell, h_i is distance between the cell i and the attached surface, and $h_{\max}$ is the maximum biofilm thickness at that time point.

Nutrient-limited detachment

It is known that when nutrient becomes limited, cells tend to detach from the original locations (5,27,28). Nutrient-limited detachment mechanism relates cell detachment process with local nutrient concentration rather than biofilm thickness. The lower the local nutrient concentration is, the higher the probability of the bacteria to be detached. The detachment probability of bacteria caused by nutrient-limited (P_{dn}) (19,27) is modeled as:

$$P_{dn} = K_{dn} \cdot \Delta t \cdot \left(1 - \frac{s_i}{s_{bulk}} \right) \tag{4}$$

where K_{dn} is the detachment coefficient, s_i is the substrate concentration at the location of the bacterium i, and s_{bulk} is the bulk nutrient concentration. It should be noted that more than one nutrient type may exist in experiments, like oxygen and carbon, but only one was considered limiting the bacterial growth in current study for simplicity. For multiple nutrients, the equation should be modified and the detachment probability should be obtained by multiplying the influence of each nutrient.

Erosion detachment

In biofilms, bacteria are encapsulated in matrix and constrained by all kinds of interactions between bacteria and nearby bacteria or extracellular polymeric substance (EPS). Bacteria on the biofilm surface (either inside or outside surface) have fewer neighbors, thus weaker interactions and easier to get detached. Erosion detachment mechanism reflects the different detachment difficulty degrees of surface bacteria and bacteria embed deep in biofilms. The detachment probability (P_{de}) of a bacterium caused by weak interactions (19) could be modeled as:

$$P_{de} = K_{de} \cdot \Delta t \cdot \left(\frac{NB_{free,i}}{NB_{total}} \right) \tag{5}$$

where K_{de} is the detachment coefficient, $NB_{free,i}$ is the number of neighbor grids free of biomass, and NB_{total} is the total number of neighbor grids.

After the calculations, detachment probabilities (P_{ds}, P_{dn}, and P_{de}) were compared with a random number uniformly distributed between 0 and 1 to determine whether the cell should be detached.

Parameters in Simulation

Model parameters

All bacterial growth relevant parameters (TABLE 1) used in the simulation were chosen according to literatures (18,19), which are applicable to single species *Pseudomonas aeruginosa* biofilm growth in a flow cell.

Biofilm characterization parameters

Two groups of parameters were applied. One group, including biofilm average and maximum thickness and cell number inside biofilms, was applied to indicate the biofilm growth conditions. The other group, which includes biofilm surface coverage, enlargement, and surface roughness, was used to evaluate biofilm morphology complexity.

TABLE 1. Parameters used in the simulations

Parameters	Values	Units
Size of computation domain	200x200x200	μm^3
Size of each grid	4x4x4	μm^3
Bulk concentration of substrate	0.04	$g.L^{-1}$
Diffusion coefficient of substrate	$4.5x10^{-6}$	$m^2.day^{-1}$
Mass transfer boundary layer thickness	20	μm
Initial number of cells	10	
Maximum specific growth rate	0.625	$hour^{-1}$
Substrate half-saturation coefficient	0.02	$g.L^{-1}$
Yield biomass on substrate	0.2	$g.g^{-1}$
Average cell radius at division	2	μm
Simulation time step	1	hour
Shear detachment coefficient#	0.05/0.1/0.15	h^{-1}
Nutrient-limited detachment coefficient#	0.001/0.005/0.01	h^{-1}
Erosion detachment coefficient#	0.025/0.05/0.1	h^{-1}

(#): Three different levels of detachment coefficients from slow detachment to fast detachment were used

TABLE 2. Biofilm surface characterization parameters

Characterization parameters	Equation
Surface coverage (C)	$C = \frac{A_{cell}}{A_{surface}}$ (¥)
Surface enlargement (E)	$E = \frac{A_s}{A_p}$ (*)
Surface roughness (R)	$R = \frac{\sum_{j,k} \lvert h_{j,k} - \bar{h} \rvert}{j \cdot k}$ (Ɛ)

(¥): A_{cell} is the area of the attachment surface that is occupied by bacteria and $A_{surface}$ is the whole area of the attachment surface.

(*): A_s is the area of biofilm surface and A_p is the area of attachment surface which are attached by bacteria.

(Ɛ): $h_{j,k}$ is biofilm thickness at grid referred to as (j, k) (j is the jth grid in y direction and k is the kth grid in z direction) and $\bar{h}$ is the average biofilm thickness.

Results and Discussion

The biofilm simulations with no detachment events were treated as the control. And the three replicates used different initial bacterial locations but identical numbers. All simulations lasted 400 hours. Results of the simulations were evaluated both qualitatively by 3D structures and quantitatively by characterization parameters.

Biofilm 3D Structures

Representative biofilm structures at 200 hours and 400 hours are shown (Figure 2 and Figure 3). The two time points were chosen to represent the two biofilm development stages before and after the detachment became significant. Similar biofilm structures as the control (Figure 2A) were observed at 200 hours under shear detachment regardless of the detachment coefficient values applied (Figure 2B-2D). However, at 400 hours, shear detachment, especially when large detachment coefficient values applied, showed significant influence on thinning the biofilms (Figure 3B-3D). More isolated cluster structures were formed under nutrient-limited detachment at 200 hours (Figure 2E-2G) due to the detachment of the bacteria around the attachment surfaces, and for the same reason at 400 hours, the weakened attachment (Figure 3F, 3G) of biofilms to the attachment surfaces led to the detachment of large amount of biomass (Figure 3G), which could be defined as sloughing events. For erosion detachment, no significant effect could be found throughout the simulation period (Figure 2H and Figure 3H) when applying the smallest coefficient value. But when erosion detachment coefficient is large enough, influence of it started to be observable at 200 hours (Figure 2J and Figure 3J). When all three detachment mechanisms were added at the same time, even all three detachment coefficients were chosen to be the smallest ones, influence of detachment on biofilm structure could be clearly seen (Figure 3K). When large enough detachment coefficients were chosen, erosion detachment led to the formation of larger clusters and nutrient-limited detachment resulted into the hollow structure formation before sloughing event (Figure 3M).

Under the current settings, the 3D biofilm structure results indicate that shear and nutrient-limited detachment only show effects at relative later stages of biofilm development, while erosion detachment starts to influence biofilm structure formation from the beginning of biofilm development. From the definitions of the detachment mechanisms, it is clear that the thicker the biofilm, the higher shear detachment. Similarly, nutrient limitation is more likely to be reached inside large clusters at the late stage of biofilm development to promote nutrient-limited detachment. On the other hand, the definition of erosion detachment does not depend on biofilm thickness, thus can happen at the early stage of biofilm growth.

The above observations show that shear detachment made the biofilm thinner, nutrient-limited detachment formed holes near the biofilm attached surface, and erosion detachment led to formation of separated bacterial clusters, which are the similar trends as the previous BBM results (19). Thus, the feasibility to study biofilm detachment using the IBM method (iDynoMiCs) was proved. Furthermore, the above results also showed that the significance of each detachment mechanisms is time dependent, i.e., depending on the stage of biofilm development.

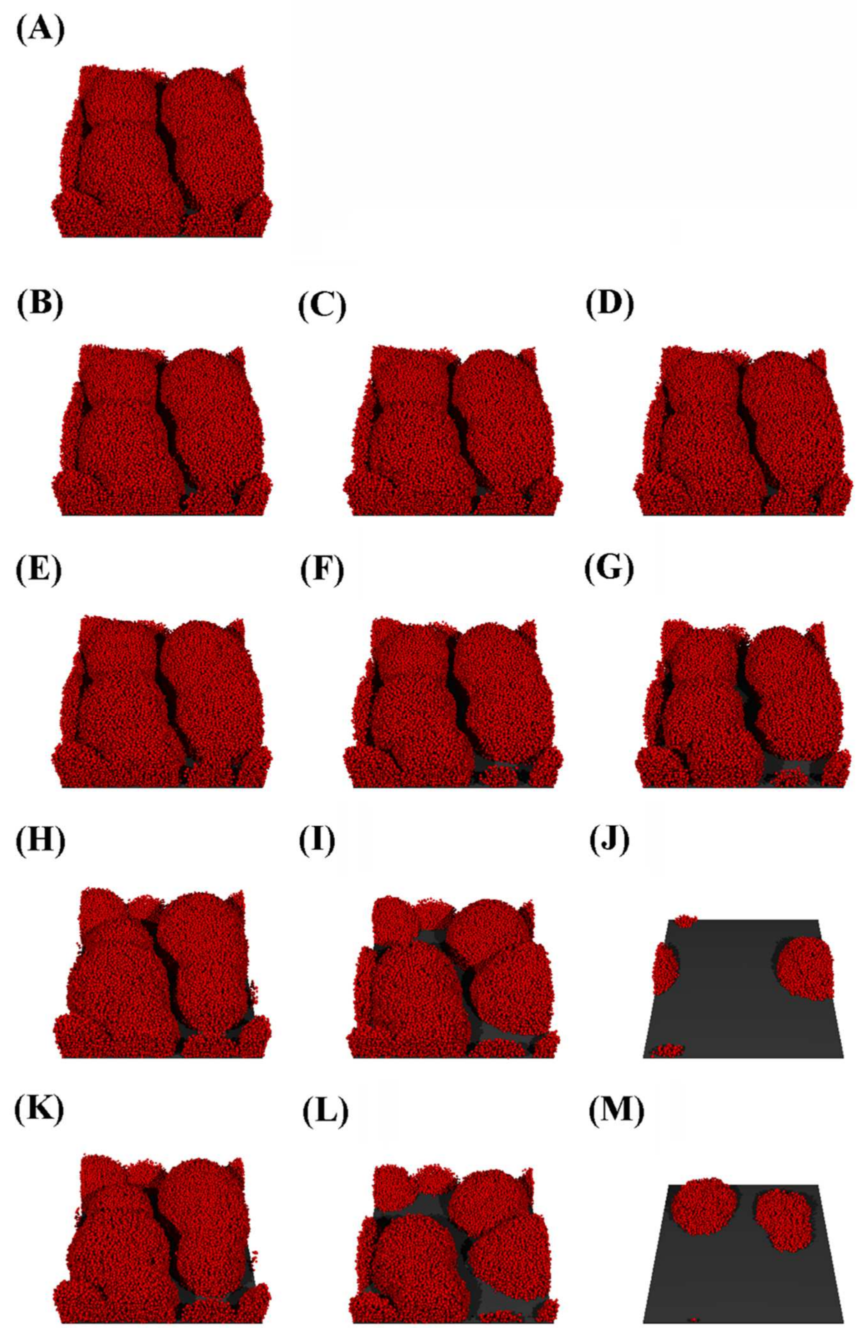

Figure 2. Biofilm structures at 200 hours ((A): without detachment; (B, C, D): with shear detachment coefficient of 0.05, 0.1, 0.15, respectively; (E, F, G): with nutrient-limited detachment coefficient of 0.001, 0.005, 0.01, respectively; (H, I, J): with erosion detachment coefficient of 0.025, 0.05, 0.1; (K, L, M): with all three detachment but with all three smallest coefficients, all three middle coefficient values, and all three largest coefficients respectively)

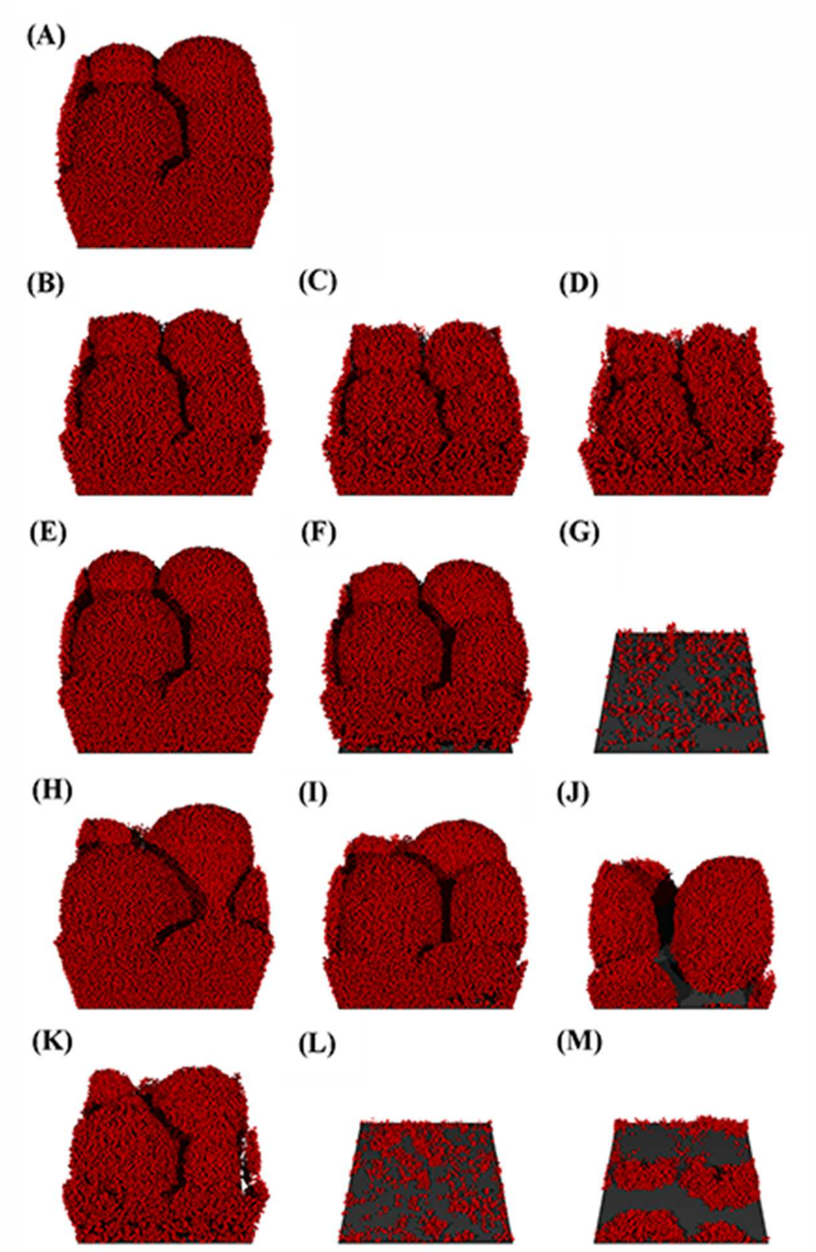

Figure 3. Biofilm structures at 400 hours ((A): without detachment; (B, C, D): with shear detachment coefficient of 0.05, 0.1, 0.15, respectively; (E, F, G): with nutrient-limited detachment coefficient of 0.001, 0.005, 0.01, respectively; (H, I, J): with erosion detachment coefficient of 0.025, 0.05, 0.1; (K, L, M): with all three detachment but with all three smallest coefficients, all three middle coefficient values, and all three largest coefficients respectively)

Biofilm detachment and growth characterization

Along with biofilm development, detachment rate also changed from time to time (Figure 4). For shear and nutrient-limited detachment, equilibrium detachment rate states could be reached (Figure 4A and Figure 4B). Big vibrations in the equilibrium detachment rate could happen at later stages for nutrient-limited detachment, which could be attributed to sloughing events (Figure 4B). For erosion detachment, the detached cell number kept increasing with time rather than reached equilibrium states in the whole simulation period (Figure 4C). When all three detachment mechanisms were added, complicated behaviors were observed depending on the coefficient values chosen. When all smallest values were chosen (‘All min’ condition in Figure 4D), detached cell number kept increasing very fast. But when the three coefficients were all set to the maximum values (All max in Figure 4D), detached cell number first increase and then decrease then maintain the smallest values due to the small biomass left on the surface. The increase and then decrease phenomena was also observed for the condition when the coefficients were set to the medium values. This turning of detached cell number trend could be attributed to the result of sloughing events, which are more likely to happen when the coefficients are larger.

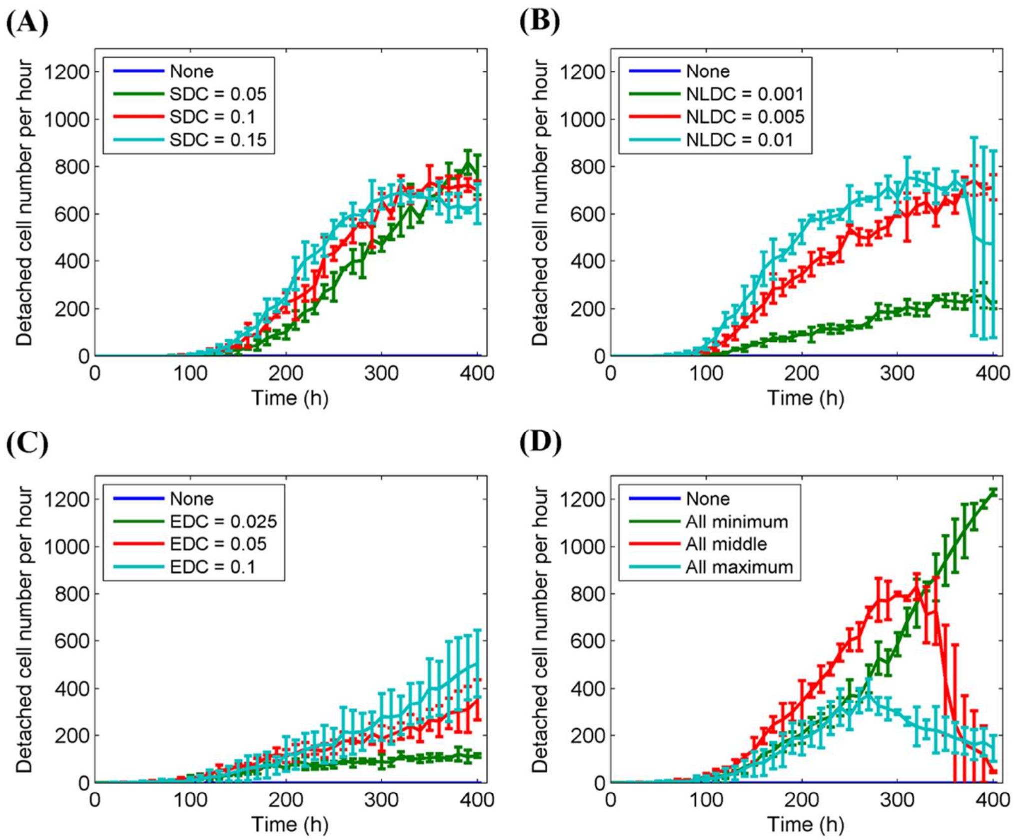

Figure 4. Detached cell number under different detachment mechanisms ((A) – different shear detachment coefficients (SDC), (B) – different nutrient-limited detachment coefficients (NLDC), (C) –different erosion detachment coefficients (EDC), and (D) – all three detachment, where 'All minimum' refers to SDC = 0.05, NLDC = 0.001, and EDC = 0.025, 'All middle' refers to SDC = 0.1, NLDC = 0.005, and EDC = 0.05, and 'All maximum' refers to SDC = 0.15, NLDC = 0.01, and EDC = 0.1. Same captions were applied for the following figures.)

Total cell number inside the biofilms was used as an indication of the bacterial growth and all dead bacteria were excluded. For shear detachment, instead of reaching equilibrium states, decreases of cell number after reaching the maximum values were observed (Figure 5A). Nutrient-limited detachment could lead to either continuous increasing or equilibrium states of total cell number inside biofilms before reaching sloughing events (Figure 5B) for the time period chosen in the current study. If the study time period could be extended long enough, the growth of bacteria will slowly reach the steady state followed by sloughing independent of the coefficient values. For erosion detachment, the cell number kept increasing with slower speeds than the control (Figure 5C). When all three detachment mechanisms are enabled at the same time, the similar trend was observed as the adding of only shear detachment, but the absolute cell number values are relative smaller as a result of the adding of the other two detachment mechanisms (Figure 5D). With detailed inspection and comparison between Figure 5D with Figure 5C, it could be observed that in the initial growth period, from 0 to 100 hours, the total cell number of biofilms when all three detachment mechanisms were added showed exactly same values as the biofilms formed with adding of only erosion detachment, which could led to the conclusion that erosion detachment showed the most significant influence in this stage. After that, from 100 hours, effect of shear and nutrient-limited detachment became obvious and the total cell number of biofilms enabled all three detachment mechanisms showed complex combined result of biofilms formed with each one detachment mechanism.

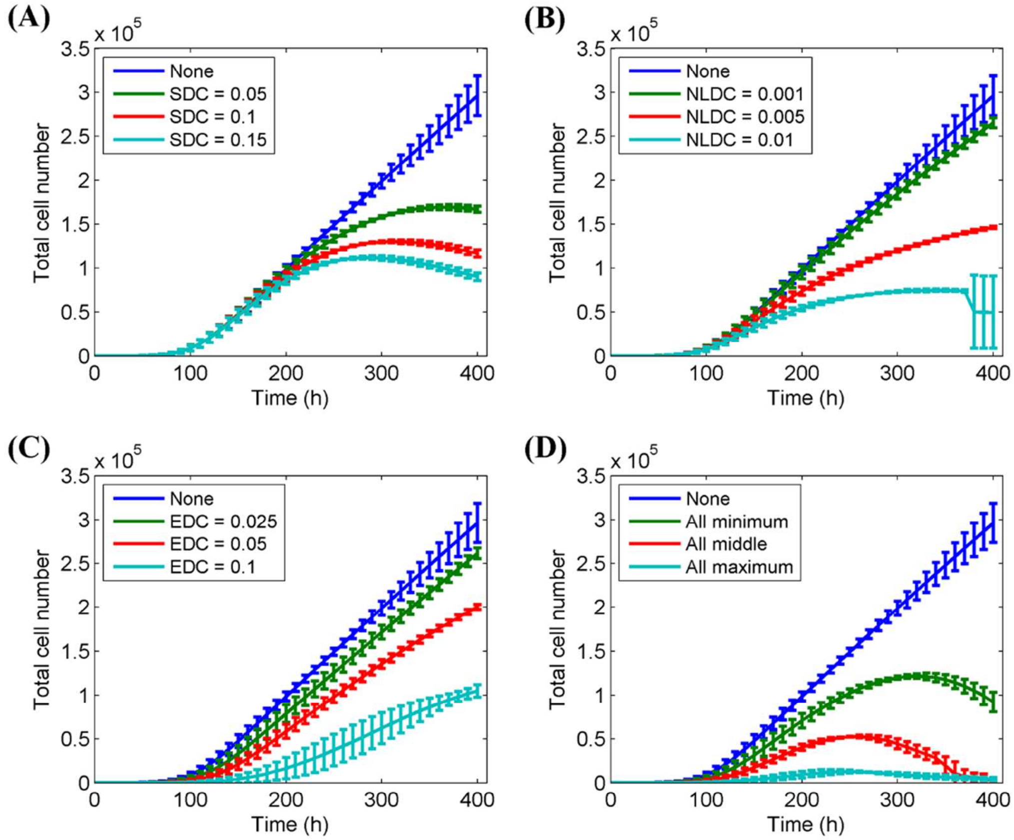

Figure 5. Total cell number inside biofilms

Maximum thickness is the distance between the attachment surface and biofilm top surface. Maximum thickness of the control kept increasing almost linearly while a trend to reach equilibrium maximum thickness values was shown when shear detachment was included (Figure 6A). Nutrient-limited detachment could only happen when bacteria are embedded inside biofilm clusters. Therefore, as expected, maximum biofilm thickness was not influenced much by nutrient-limited detachment before sloughing events (Figure 6B). For erosion detachment, maximum biofilm thickness showed continuous increasing similar to control but with relatively slower increasing rates (Figure 6C) which could relate to the definition of erosion detachment that the bacteria in the thin surface layer of biofilms have higher probability to get detached by this mechanism. As such, the maximum thickness of these biofilms kept increasing but increased more slowly.

Average thickness of biofilms with only shear detachment showed similar trend as their maximum thickness values but with much more observable equilibrium state (Figure 7A). The time point when biofilm reached equilibrium state, which is around 200 hours, was independent of the detachment coefficient values. The achievement of biofilm steady state when shear detachment is defined as a quadratic dependency on biofilm thickness has been previously reported (15) and widely accepted. Average thickness of biofilms with only nutrient-limited detachment first increased before reaching a short equilibrium state; then increased again until sloughing events happened (Figure 7B). When erosion detachment was enabled alone, continuous increasing of average thickness was observed (Figure 7C) without the trend of reaching equilibrium state. When all three detachment mechanisms were included, average thickness first increased and decreased after reaching a turning point for the largest detachment coefficient condition; for the other two conditions, average thickness first reached a short equilibrium state and then increase again, which was similar to biofilms formed with only nutrient-limited detachment (Figure 7D).

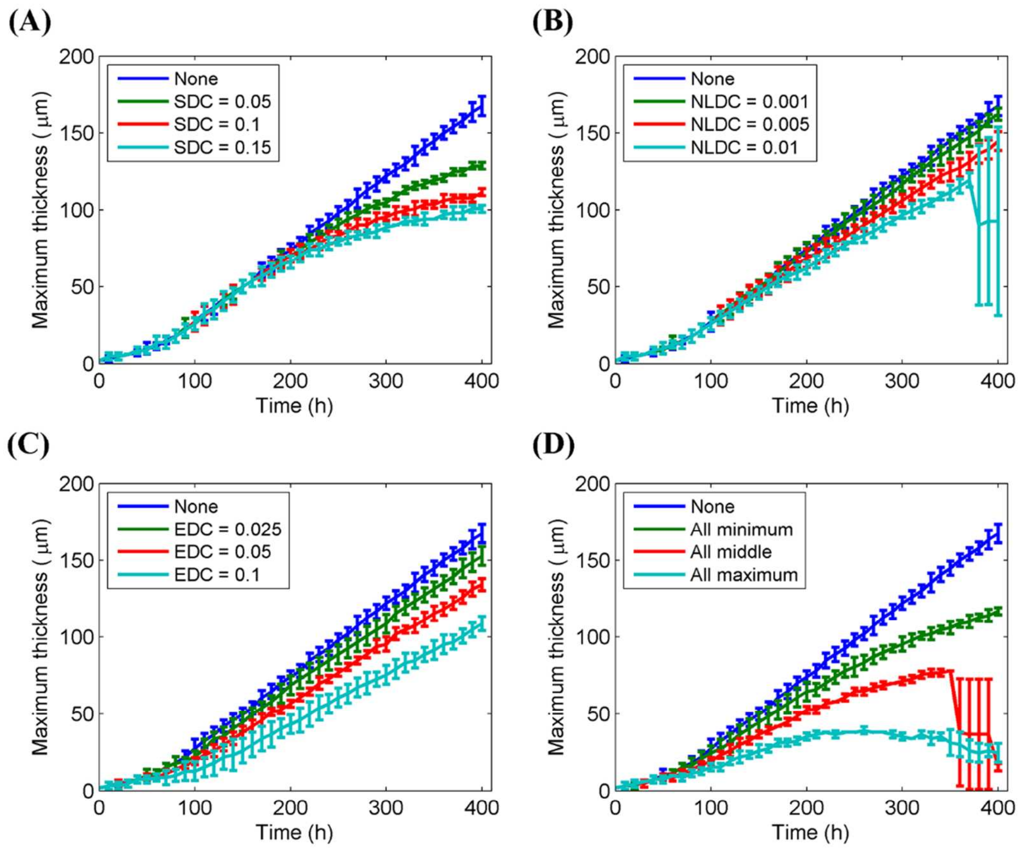

Figure 6. Biofilm maximum thickness

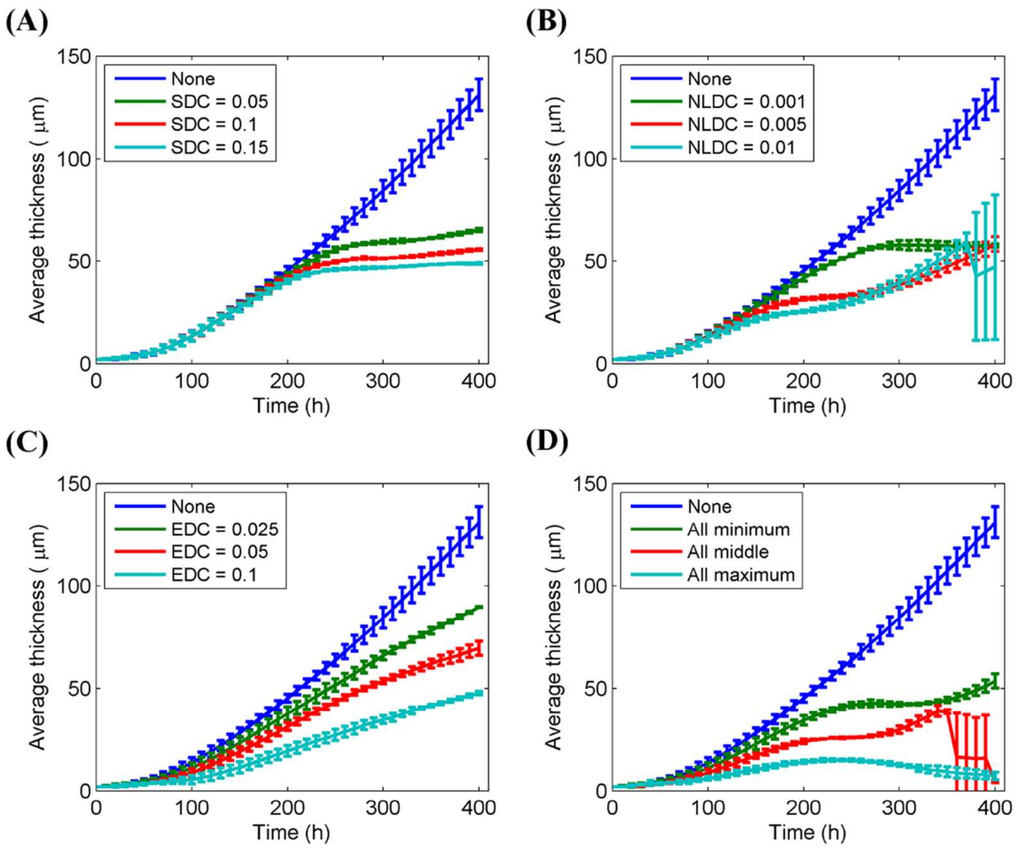

Figure 7. Biofilm average thickness

Biofilm surface characterization

In order to compare the biofilm surface properties, surface parameters as explained before were calculated and evaluated. Surface coverage as defined can indicate the coverage of the biofilm on the surface. Shear detachment mainly influences biofilm top surface and no obvious effect on biofilm surface coverage could be observed (Figure 8A). Nutrient-limited detachment, on the other hand, is a process which starts specifically from the deep inner biofilm parts where nutrient cannot penetrate to. Thus it showed significant influence on decreasing the biofilm surface coverage when nutrient started to limit bacteria growth (Figure 8B). Erosion detachment had only minor effect on decreasing surface coverage during early biofilm formation period but at last all surface would be covered by biofilms (Figure 8C). As a combination, biofilms formed under all three detachment mechanisms showed different trends under different coefficient value sets (Figure 8D), which could be linked to the importance of each detachment mechanism. Shear detachment showed no contribution, while erosion detachment showed the leading role at the early stages (before 200 hours) and nutrient-limited showed more important effect at the later stages (after 200 hours).

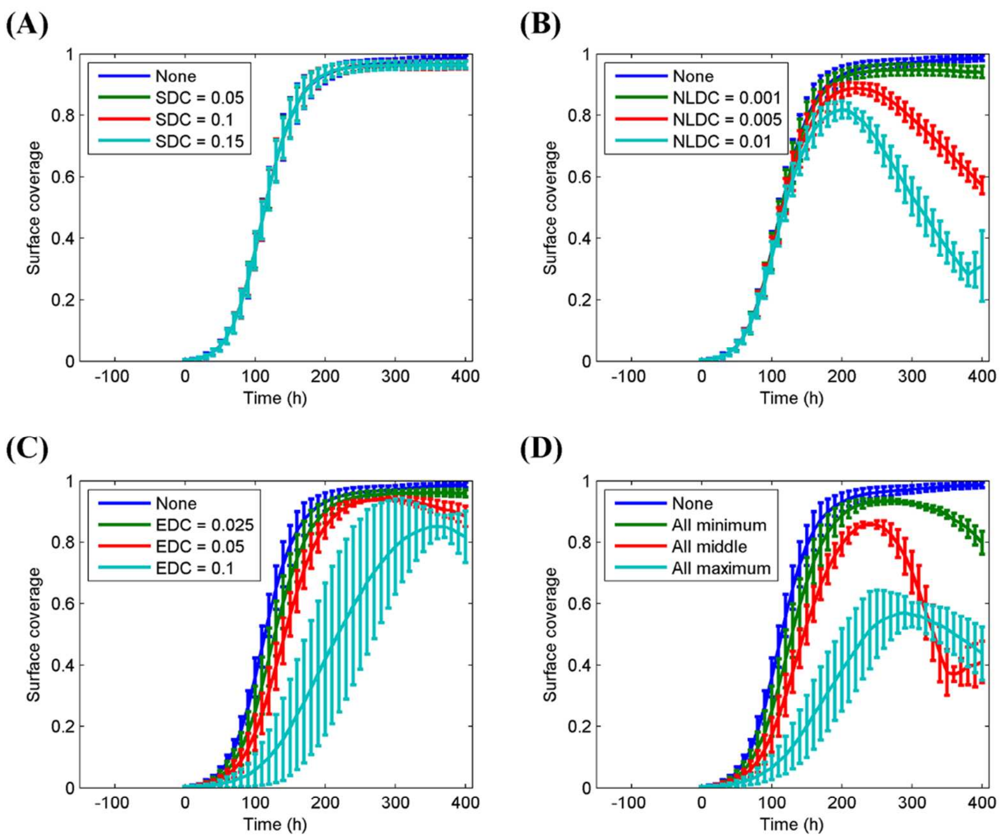

Figure 8. Biofilm surface coverage

Surface enlargement values of biofilms under shear detachment were increased at late stages mainly because of the loosely packed biofilm surface layers (Figure 9A). The surface enlargement of biofilms under nutrient-limited detachment increased a lot compared with control and this could be the result of decreased surface coverage due to the detachment of bacteira near the attachment surface (Figure 9B). Biofilm under erosion detachment also showed increased enlargement values (Figure 9C), which is expected because erosion helped the formation of more isolated bacterial clusters. When all three detachment mechanisms were enabled, there was a turning point, which depended on the detachment coefficient chosen, after which surface enlargement started to decrease (Figure 9D).

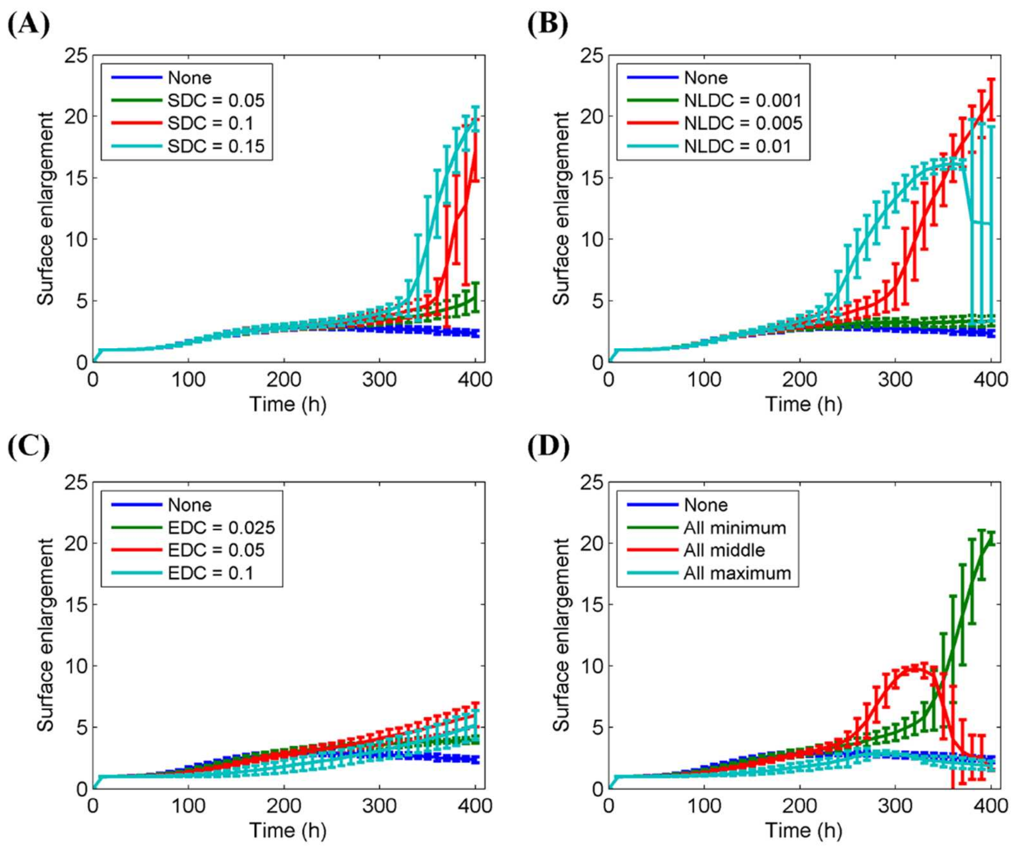

Figure 9. Biofilm surface enlargement

Lastly, biofilm surface roughness was evaluated. Surface roughness of the control mainly increased and then reached a threshold value. Surface roughness of biofilms with shear detachment first increased with slower speed and reached a short equilibrium state and then increased again (Figure 10A). It is worthwhile to suspect that the shear smooth effect could only be maintained in a short time period only, after which the biofilms with shear detachment could possibility be rougher even than the control. This later increase of surface roughness could also be the result of the loosely packed surface layers of biofilms, similar to the surface enlargement. Nutrient-limited detachment didn't show any conclusive influence on surface roughness (Figure 10B), which is understandable as nutrient-limited influence very little on biofilm surface properties. Surface roughness of biofilms under erosion kept increasing linearly which was quite different form the control where the increase of surface roughness slowed down after 300 hours (Figure 10C). Therefore, it could be predicted that eventually these biofilms would become rougher than the control. When all three detachment mechanisms were applied together, the overall effect was that the larger coefficient values, the smoother the biofilms except when sloughing happened (Figure 10D).

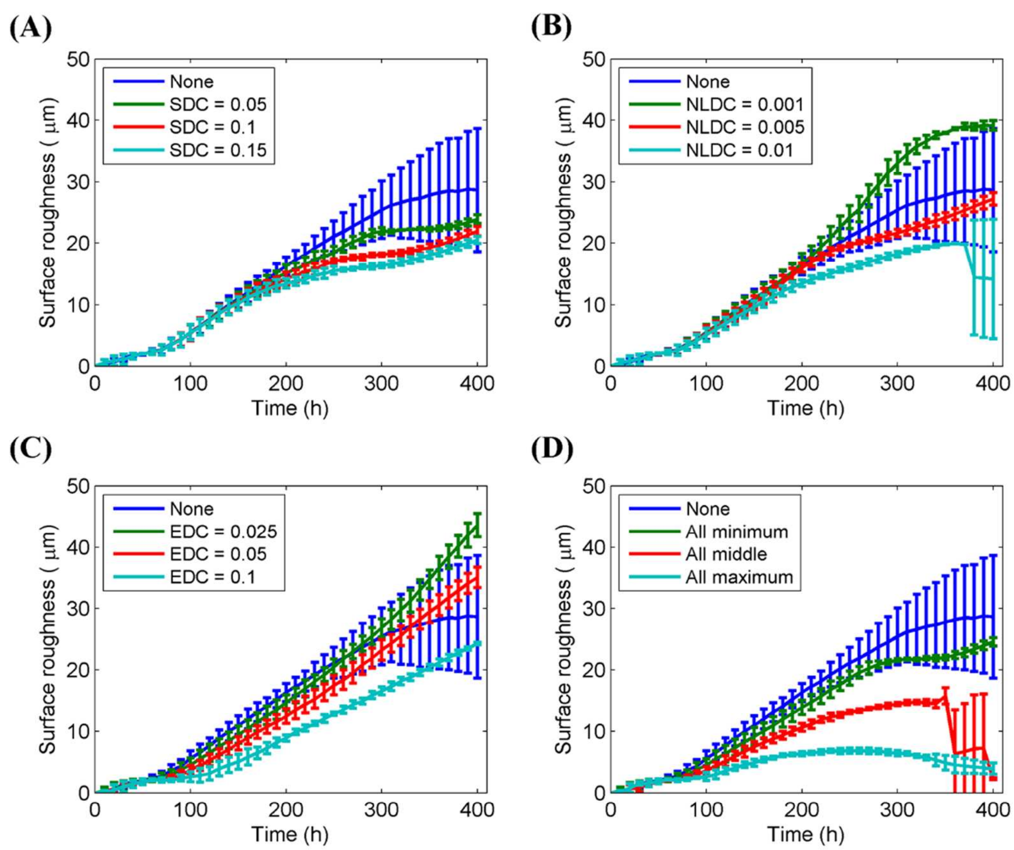

Figure 10. Biofilm surface roughness

Interestingly, it is found that for parameters like total cell number, average thickness and roughness, variations among replicates with one or more detachment mechanisms enabled were much smaller than the control in all the simulations, which means that these parameters were more consistent and suitable to characterize biofilm structure properties, while other parameters, like maximum thickness, surface enlargement and coverage, showed large variations. In general, there are many factors could affect the variations, or the error bars in the plots. First, the variation of initial cell attachment conditions could cause the error bar in all simulations. The initial cell number for all simulation was set to 10, but biomass of each bacterium as well as its location were chosen randomly from defined distributions, i.e., a Gaussian distribution for biomass and an even distribution for locations on the substrate. Second, the values of detachment coefficient and the time point of biofilm development affected error bars as well. When nutrient-limited detachment was effective, sloughing events were the main reason for the sudden increase of error bar values, such as Fig. 5B. If big error bars were observed for a long time period, like Fig. 8C, it was probably due to the large bacterial detachment occurred at the early stage as indicated in Fig. 5C, which led to the large variations in the subsequent biofilm development. As for the control biofilms without bacterial detachment, the error bars increased smoothly during development, which could be attributed to the colonial growth effect.

Discussion and Conclusion

Experimental work of shear effects on biofilm development has been reported in the literature (13,29–31). Some showed that the increasing of shear stress only had a temporary short-term effect and biofilms could adapt to the shear increase and return to previously established steady state after a certain time period (30). Others showed that under higher shearing, elevated detachment happened, which would result into smoother and thinner biofilms (29,31), which is similar as what was reported in this simulation. Nutrient-limited detachment was less frequently studied experimentally, but what have been found in the current study that nutrient limitation led to hollow structures in biofilm clusters and eventually, sloughing events, had been previously reported (27,32,33). Finally, erosion detachment alone was hardly evaluated, but one of the findings here that erosion detachment started to be important for biofilm formation since early biofilm development stages agrees with the previous report (34).

New findings were also discovered in current individual based simulation. First, the current study showed that different detachment mechanisms played different roles on biofilm structure formation at different biofilm development stages. To be specific, erosion detachment was more important at early biofilm stages while shear detachment was more important at later stages and nutrient-limited detachment only showed influence when biofilm clusters became large enough to create thick nutrient diffusion barrier. Second, different detachment mechanism has different sensitivities on the selection of detachment coefficient values in the current study. Particularly, shear detachment always showed similar effects on biofilm formation regardless of the coefficient values chosen. Considering that shear detachment only significantly affected biofilm structure at the later stage, this result indicated that the initial conditions of a biofilm may play a significant role in the development of biofilm structure, which is well known for a chaotic system, i.e., the butterfly effect. For Nutrient-limited detachment, depending on the coefficient value, sloughing events could happen early or late. For the erosion detachment, its influence on biofilm formation depends very much on the coefficient values. Lastly, with detachment enabled, all biofilm parameters, except some conditions discussed before, had smaller error bars than the biofilms formed without detachment, i.e., detachment could help form more reproducible biofilms when compared with biofilms formed without detachment.

In summary, biofilms development under different detachment mechanisms were successfully simulated using the individual based modeling method. Both 3D observations and structural parameters were evaluated, which showed different influence of these detachments on biofilm development and structural evolution. Finding in the current simulation were compared with previous experimental and numerical results whenever available. New findings are also discovered including the effects of different detachment mechanisms on the equilibrium state, time-dependent effects of each detachment mechanism on biofilm structure, sensitivity of the detachment coefficient values, etc.

Acknowledge

Y. Z. acknowledges the Tier-1 Academic Research Funds from the Singapore Ministry of Education (RGT 30/13, RGC 6/13 and RGC 1/14).

References

1. Yun M, Yeon K, Park J, Lee C, Chun J. Characterization of biofilm structure and its effect on membrane permeability in MBR for dye wastewater treatment. 2006;40:45–52.

2. Lazarova V, Manem J. Biofilm characterization and activity analysis in water and wastewater treatment. Water Res. 1995;29(10):2227–45.

3. Costerton JW. Bacterial Biofilms: A Common Cause of Persistent Infections. Science (80-) [Internet]. 1999 May 21 [cited 2014 Jul 10];284(5418):1318–22. Available from: http://www.sciencemag.org/cgi/doi/10.1126/science.284.5418.1318

4. Vallet I, Diggle SP, Stacey RE, Ventre I, Lory S, Lazdunski A, et al. Biofilm formation in Pseudomonas aeruginosa : fimbrial cup gene clusters are controlled by the transcriptional regulator MvaT. J Bacteriol. 2004;186(9):2880–90.

5. Allison DG. The biofilm matrix. Biofouling. 2003;19(2):139–50.

6. Picioreanu C, van Loosdrecht MC, Heijnen JJ. Mathematical modeling of biofilm structure with a hybrid differential-discrete cellular automaton approach. Biotechnol Bioeng [Internet]. 1998 Apr 5;58(1):101–16. Available from: http://www.ncbi.nlm.nih.gov/pubmed/10099266

7. Stoodley P, Boyle JD, DeBeer D, Lappin□Scott HM. Evolving perspectives of biofilm structure. Biofouling [Internet]. 1999 Jun [cited 2014 Aug 29];14(1):75–90. Available from: http://www.tandfonline.com/doi/abs/10.1080/08927019909378398

8. Wijeyekoon S, Mino T, Satoh H, Matsuo T. Effects of substrate loading rate on biofilm structure. Water Res [Internet]. 2004 May [cited 2014 Aug 21];38(10):2479–88. Available from: http://www.ncbi.nlm.nih.gov/pubmed/15159151

9. Møller S, Pedersen a R, Poulsen LK, Arvin E, Molin S. Activity and three-dimensional distribution of toluene-degrading Pseudomonas putida in a multispecies biofilm assessed by quantitative in situ hybridization and scanning confocal laser microscopy. Appl Environ Microbiol [Internet]. 1996 Dec;62(12):4632–40. Available from: http://www.pubmedcentral.nih.gov/articlerender.fcgi?artid=168289&tool=pmcentrez&rendertype=abstract

10. A unifying hypothesis for te structure of microbial biofilms based on cellular automaton models.pdf.

11. Dalton HM, Poulsen LK, Halasz P, Angles ML, Goodman a E, Marshall KC. Substratum-induced morphological changes in a marine bacterium and their relevance to biofilm structure. J Bacteriol [Internet]. 1994 Nov;176(22):6900–6. Available from: http://www.pubmedcentral.nih.gov/articlerender.fcgi?artid=197059&tool=pmcentrez&rendertype=abstract

12. Li B, Logan BE. Bacterial adhesion to glass and metal-oxide surfaces. Colloids Surf B Biointerfaces [Internet]. 2004 Jul 15 [cited 2014 Jul 14];36(2):81–90. Available from: http://www.ncbi.nlm.nih.gov/pubmed/15261011

13. Peyton BM. Effects of shear stress and substrate loading rate on Pseudomonas aeruginosa biofilm thickness and density. Water Res. 1996;30(1):29–36.

14. Stoodley P, Boyle JD, Lappin-scott HM. Influence of flow on the structure of bacterial biofilms. 1999;

15. Stewart PS. A model of biofilm detachment. Biotechnol Bioeng. 1993;41(1):111–7.

16. Van Loosdrecht MCM, Eikelboom D, Gjaltema A, Mulder A, Tijhuis L, Heihnen JJ. Biofilm structures. Water Sci Technol. 1995;32(8):35–43.

17. Xavier JDB, Picioreanu C, van Loosdrecht MCM. A general description of detachment for multidimensional modelling of biofilms. Biotechnol Bioeng [Internet]. 2005 Sep 20 [cited 2014 Jul 10];91(6):651–69. Available from: http://www.ncbi.nlm.nih.gov/pubmed/15918167

18. Picioreanu C, Kreft J-U, Klausen M, Haagensen J a. J, Tolker-Nielsen T, Molin S. Microbial motility involvement in biofilm structure formation – a 3D modelling study.

Water Sci Technol [Internet]. 2007 May [cited 2014 Aug 9];55(8-9):337. Available from: http://www.iwaponline.com/wst/05508/wst055080337.htm

19. Chambless JD, Stewart PS. A RTICLE A Three-Dimensional Computer Model Analysis of Three Hypothetical Biofilm Detachment Mechanisms. 2007;97(6):1573–84.

20. Martin KJ, Picioreanu C, Nerenberg R. Multidimensional modeling of biofilm development and fluid dynamics in a hydrogen-based , membrane biofilm reactor (MBfR). Water Res [Internet]. Elsevier Ltd; 2013;47(13):4739–51. Available from: http://dx.doi.org/10.1016/j.watres.2013.04.031

21. Picioreanu C, Loosdrecht MCM Van, Heijnen JJ. Two-dimensional model of biofilm detachment caused by internal stress from liquid flow. Biotechnol Bioeng. 2001;72(2):205–18.

22. Lardon LA, Merkey B V, Martins S, Dötsch A, Picioreanu C, Kreft J, et al. iDynoMiCS : next-generation individual-based modelling of biofilms. 2011;13:2416–34.

23. Picioreanu C, van Loosdrecht MC, Heijnen JJ. A new combined differential-discrete cellular automaton approach for biofilm modeling: application for growth in gel beads. Biotechnol Bioeng [Internet]. 1998 Mar 20;57(6):718–31. Available from: http://www.ncbi.nlm.nih.gov/pubmed/10099251

24. Picioreanu C, Loosdrecht MCM Van, Heijnen JJ. Multidimensional modelling of biofilm structure. 1999;

25. Kreft JU, Booth G, Wimpenny JW. BacSim, a simulator for individual-based modelling of bacterial colony growth. Microbiology [Internet]. 1998 Dec;144 (Pt 1:3275–87. Available from: http://www.ncbi.nlm.nih.gov/pubmed/9884219

26. Kreft JU, Picioreanu C, Wimpenny JW, van Loosdrecht MC. Individual-based modelling of biofilms. Microbiology [Internet]. 2001 Nov;147(Pt 11):2897–912. Available from: http://www.ncbi.nlm.nih.gov/pubmed/11700341

27. Hunt SM, Werner EM, Huang B, Hamilton A, Stewart PS, Hamilton MA. Hypothesis for the role of nutrient starvation in biofilm detachment. Appl Environ Microbiol. 2004;70(12):7418–25.

28. O'Toole G, Kaplan HB, Kolter R. Biofilm formation as microbial development. Annu Rev Microbiol [Internet]. 2000 Jan;54:49–79. Available from: http://www.ncbi.nlm.nih.gov/pubmed/11018124

29. Pei-shi QI, Wen-bin W, Zheng QI. Effect of Shear Stress on Biofilm Morphological Characteristics and the Secretion of Extracellular Polymeric Substances. 2008;3438–41.

30. Choi YC, Morgenroth E. Monitoring biofilm detachment under dynamic changes in shear stress using laser-based particle size analysis and mass fractionation. Water Sci Technol [Internet]. 2003 Jan;47(5):69–76. Available from: http://www.ncbi.nlm.nih.gov/pubmed/12701909

31. Manz B, Volke F, Goll D, Horn H. Investigation of biofilm structure, flow patterns and detachment with magnetic resonance imaging. Water Sci Technol. 2005;52(7):1–6.

32. Gjermansen M, Ragas P, Sternberg C, Molin S, Tolker-Nielsen T. Characterization of starvation-induced dispersion in Pseudomonas putida biofilms. Environ Microbiol. 2005;7(6):894–904.

33. Gjermansen M, Nilsson M, Yang L, Tolker-Nielsen T. Characterization of starvation-induced dispersion in Pseudomonas putida biofilms: Genetic elements and molecular mechanisms. Mol Microbiol. 2010;75(4):815–26.

34. Bester E, Wolfaardt G, Joubert L, Garny K, Saftic S. Planktonic-cell yield of a pseudomonad biofilm. Appl Environ Microbiol. 2005;71(12):7792–8.